



Unveiling the nature of Seyfert nuclei with 1 - 100 micron spectral energy distributions

C.L. Buchanan¹, J.F. Gallimore², C.P. O’Dea³, S.A. Baum⁴, D.J. Axon³, A. Robinson³,
J. Noel-Storr³, A. Yzaguire², M. Elitzur⁵, M. Elvis⁶, and C. Tadhunter⁷

¹ University of Melbourne, Victoria, 3010, Australia e-mail: clb@unimelb.edu.au

² Bucknell University, Lewisburg, PA, 17837, USA

³ Rochester Institute of Technology, 84 Lomb Memorial Drive, Rochester, NY, 14623, USA

⁴ Rochester Institute of Technology, 54 Lomb Memorial Drive, Rochester, NY, 14623, USA

⁵ University of Kentucky, Lexington, KY, 40506, USA

⁶ Harvard-Smithsonian Center for Astrophysics, 60 Garden Street, Cambridge, MA, 02138, USA

⁷ University of Sheffield, Sheffield, S3 7RH, UK

Abstract. The infrared is a key wavelength regime for probing the dusty, obscured nuclear regions of active galaxies. We present results from an infrared study of 87 nearby Seyfert galaxies using the Spitzer Space Telescope and ground-based telescopes. Combining detailed modelling of the 3 - 100 micron spectral energy distributions with mid-IR spectral diagnostics and near-infrared observations, we find broad support for the unified model of AGNs. The IR emission of Seyfert 1s and 2s is consistent with their having the same type of central engine viewed at a different orientation. The nature of the putative torus is becoming clearer; in particular we present evidence that it is likely a clumpy medium. Mid-infrared correlations between tracers of star formation and AGN ionizing luminosity reveal the starburst-AGN connection implied by the black hole/bulge mass relation, however it is not yet clear if this is due to feedback.

Key words. Galaxies: Seyfert – Galaxies: Active – Galaxies: Stellar content – Infrared: galaxies

1. Introduction

The infrared wavelength regime provides a unique probe into the nuclear regions of active galaxies (AGNs), as the circumnuclear dust absorbs and reradiates higher energy photons from the nucleus. We are conducting a study of the infrared emission from nearby Seyfert galaxies, using the Spitzer Space Telescope

and ground-based telescopes (Buchanan et al. 2006). The goal is to construct matched-aperture infrared (IR) spectral energy distributions (SEDs) of the central few kiloparsecs of a large sample of nearby Seyfert galaxies, and to decompose the SEDs into the contributions to the dust heating from the active nucleus and any circumnuclear starburst.

2. Seyfert infrared SEDs

The sample of objects studied comprises the 85 Seyfert galaxies from the extended $12\ \mu\text{m}$ sample (Rush et al. 1993) with $cz < 10000\text{kms}^{-1}$, excluding two sources due to problems with the data. The properties of the sample are discussed in more detail in (Buchanan et al. 2006) and Baum et al. (2008, in preparation). The Spitzer SEDs cover the wavelength range $3.6 - 100\ \mu\text{m}$, and comprise IRAC photometry at $3.6, 4.5, 5.8$ and $8.0\ \mu\text{m}$, IRS low-resolution spectroscopy from $5 - 35\ \mu\text{m}$, and MIPS SED-mode spectra from $\sim 50 - 100\ \mu\text{m}$. In addition, near-IR photometry measured using UKIRT was used to construct higher spatial resolution SEDs from $\sim 1 - 4\ \mu\text{m}$ for 40% of the sample. Example Spitzer SEDs are shown in Figure 1.

The SEDs were decomposed into starburst and AGN contributions to the dust heating (Gallimore et al. 2007 and Gallimore et al. 2008, in preparation) by fitting the combination of a clumpy torus (Nenkova, Ivezić & Elitzur 2002) and a starburst model (Siebenmorgen & Krügel 2007). SED decompositions for the sources shown in Figure 1 are shown in Figure 2.

We find that the Seyfert 1s tend to show weak silicate emission, while the Seyfert 2s show somewhat stronger silicate in absorption. This is consistent with the unified scheme for AGN. The sample contains several ‘anomalous’ sources, including Sy 1s with silicate in absorption, Sy 2s with silicate in emission and silicate absorption at $9.7\ \mu\text{m}$ but emission at $18\ \mu\text{m}$. These features can be accounted for by the clumpy torus model but not by smooth-density torus models, providing strong support for the clumpy torus model.

Hidden Seyfert 1s (optically identified Seyfert 2s with a hidden broad line region (HBLR) observed in the infrared or polarised light) closely resemble Seyfert 1 galaxies in their infrared SEDs. This provides further support for the hypothesis of the unified scheme, that type 1 and 2 AGNs contain the same sort of central engine.

We find that the Seyfert 1s and the Seyfert 2s with known hidden broad line regions are generally AGN-dominated at $12\ \mu\text{m}$, while the

Seyfert 2s without HBLR tend to be starburst-dominated. This is likely to be a selection effect in the sample due to the mild anisotropy (about a factor of 2) of the mid-IR emission and the selection of the sample at $12\ \mu\text{m}$ (Buchanan et al. 2006).

Spectral indices in the mid-IR ($20-30\ \mu\text{m}$) and far-IR ($50-90\ \mu\text{m}$) were measured, to estimate the relative contributions of cool dust. In addition, line and continuum diagnostics were measured using PAHFIT (Smith et al. 2007). Figure 3 shows that the PAH $6.2\ \mu\text{m}$ equivalent width is correlated with the mid- and far-IR spectral indices. The fact that the PAH emission is stronger in sources with a larger cool dust contribution (redder spectral indices) argues that the cool dust is primarily heated by star formation and not the active nucleus. We also note that the Sy 2s *with* hidden broad line regions show weaker star formation (weaker PAH emission) than those *without* hidden broad line regions, suggesting that the broad line region is more difficult to detect in the presence of more star formation. Correlations between AGN and starburst tracers have been found for QSOs and Seyferts (e.g., Haas et al. 2003; Maiolino et al. 2007). Figure 4 shows the observed correlation between the $6.2\ \mu\text{m}$ PAH luminosity and the $[\text{Ne V}] 24\ \mu\text{m}$ luminosity for our sample. It is not clear if this apparent correlation is due to feedback or is simply that the both properties relate directly to the available supply of molecular gas.

The near-IR SEDs were decomposed into stellar and hot dust components using a simple non-AGN + blackbody model, where the non-AGN SED was derived from the colours of non-Seyfert galaxies in the $12\ \mu\text{m}$ sample of galaxies (Spinoglio et al. 1995) and the temperature of the blackbody was allowed to vary. We find that the dust temperatures were typically $\sim 1000\ \text{K}$, somewhat cooler than the dust sublimation temperature. Figure 5 shows the fractional contribution to the emission by the hot dust component as a function of wavelength. We find that the AGN contribution increases with wavelength and dominates by $3.7\ \mu\text{m}$. The Sy 1s show slightly larger hot dust

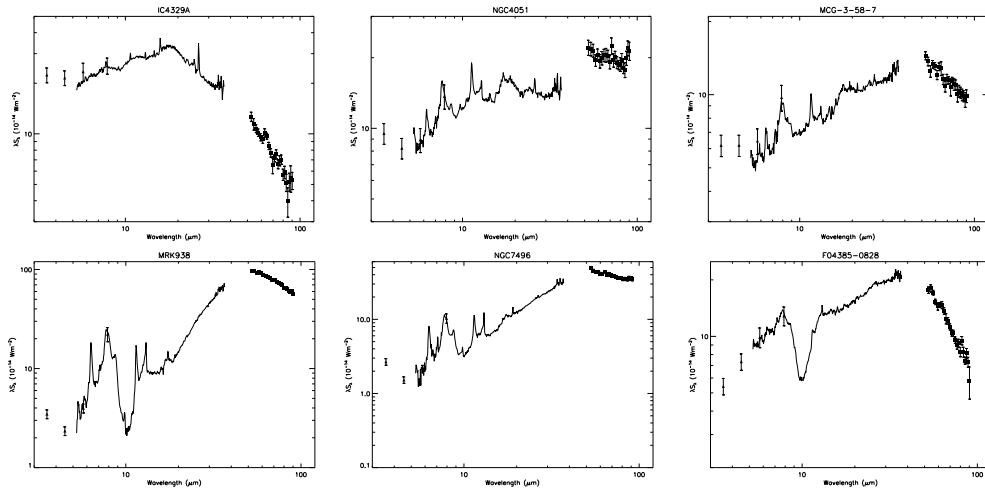


Fig. 1. Spitzer spectral energy distributions of several galaxies in the sample, illustrating the common features. Silicate features at 9.7 and 18 μm are seen weakly in emission (e.g., IC 4329A). Somewhat stronger silicate absorption is also seen, usually in conjunction with PAH emission features (e.g., MRK 938). Very strong silicate absorption (e.g., F04385-0828) is very rare in the sample, and is associated with edge-on galaxies, suggesting that some of the absorption is occurring in the host galaxy disk. PAH emission features, associated with star formation, are very common in the sample (e.g., NGC 4051, MCG -3-58-7, MRK 938, and NGC 7496). It can be seen that the mid- and far-IR spectral indices give an indication of the relative contribution of cool dust (peaking in the far-IR) to the SED: bluer slopes imply less cool dust emission.

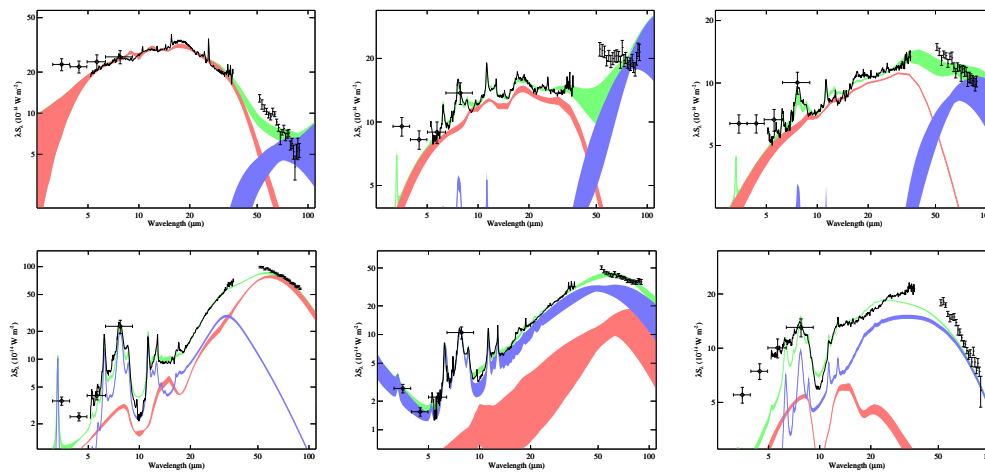


Fig. 2. SED decompositions for the objects whose SEDs are shown in Figure 1. The colored bands represent the range of SED values afforded by the acceptable fits (at 90% confidence) to the observed SED (black lines and symbols). The range of clumpy torus models is shaded red; starburst, blue; and the combination in green.

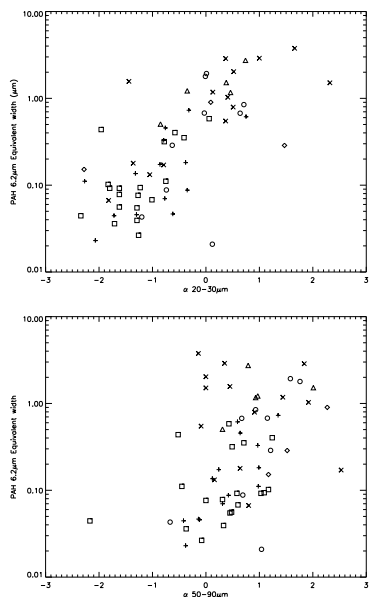


Fig. 3. PAH $6.2 \mu\text{m}$ equivalent width versus $20\text{--}30 \mu\text{m}$ spectral index (*left*) and $50\text{--}90 \mu\text{m}$ spectral index (*right*). The symbols indicate the Seyfert type: Sy 1, 1.2, 1.5, 1n (*squares*); Sy 1.8, 1.9 (*circles*); Sy 2 with hidden broad line region (*plus signs*); Sy 2 without hidden broad line region (*crosses*); LINERs (*diamond*); and starburst galaxies (*triangles*).

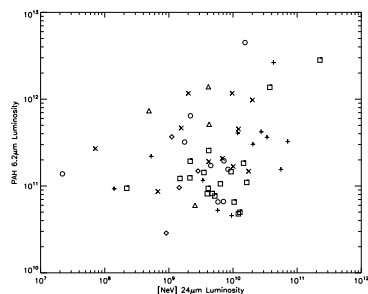


Fig. 4. PAH $6.2 \mu\text{m}$ luminosity vs [Ne V] $24 \mu\text{m}$ luminosity. The symbols are the same as for Figure 3.

contribution than the Sy 2s, as expected in the unified scheme.

3. Conclusions

We have constructed $20''$ IR SEDs of a sample of 85 nearby Seyfert galaxies. Decomposition of the SEDs into AGN and starburst contribu-

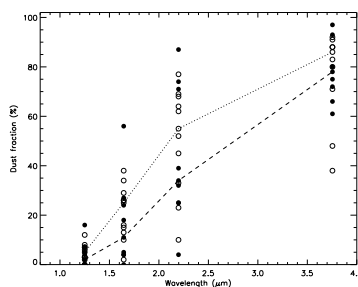


Fig. 5. Fraction of the emission contributed by the hot dust (AGN) component, at the four near-IR wavelengths observed with UKIRT. Filled symbols indicate Sy 2s and open symbols Sy 1s. The median dust fractions for type 1s and 2s are shown by the dotted and dashed lines, respectively.

tions provides support for clumpy torus models. The SEDs are consistent with the unified scheme for AGN. We find that the Seyfert 1s are AGN-dominated at $12 \mu\text{m}$ while the Seyfert 2s are starburst-dominated, which is likely to be a selection effect. We find evidence that the cool dust is primarily heated by star formation in these Seyferts.

Acknowledgements. Thanks to the organisers for a fantastic conference. This work is based in part on observations made with the Spitzer Space Telescope, which is operated by the Jet Propulsion Laboratory, California Institute of Technology under a contract with NASA. Support for this work was provided by NASA through an award issued by JPL/Caltech. The United Kingdom Infrared Telescope is operated by the Joint Astronomy Centre on behalf of the Science and Technology Facilities Council of the U.K.

References

- Buchanan, C. L., et al. 2006, *AJ*, 132, 401
- Gallimore, J. F., et al. 2007, *AAS*, 211, #46.07
- Haas, J. F., et al. 2003, *A&A*, 402, 87
- Maiolino, R., et al. 2007, *A&A*, 468, 979
- Nenkova, M., Ivezić, Ž., & Elitzur, M. 2002, *ApJ*, 570, L9
- Rush, B., Malkan, M. A., & Spinoglio, L. 1993, *ApJS*, 89, 1
- Siebenmorgen, R. & Krügel, E. 2007, *A&A*, 461, 445
- Smith, J. D., et al. 2007, *ApJ*, 656, 770
- Spinoglio, L., et al. 1995, *ApJ*, 453, 616